Observation of the Interference between the Intramolecular IR−Visible and Visible−IR Processes in the Doubly Resonant Sum Frequency Generation Vibrational Spectroscopy of Rhodamine 6G Adsorbed at the Air/Water Interface

Dan Wu,[†] Gang-Hua Deng,[‡] Yuan Guo, and Hong-fei Wang*

Beijing National Laboratory for Molecular Sciences & State Key Laboratory of Molecular Reaction Dynamics, Institute of Chemistry, the Chinese Academy of Sciences, ZhongGuanCun, Beijing, China 100190

Received: November 22, 2008

Using the picosecond visible light at 532.1 nm and infrared light at 2800−3100 cm^{-1}, we observed the interference between the intramolecular IR−visible and visible−IR processes in the doubly resonant sum frequency generation vibrational spectroscopy of Rhodamine 6G adsorbed at the air/water interface. The interference phenomenon exists for both the C−H stretching vibrations in the 2800−3100 cm^{-1} region and the skeleton vibrations in the 1450−1700 cm^{-1} region. The relative strength of the visible−IR process at different wavelengths is the result of the electronic structure of the molecule. This is the first direct observation of the visible−IR sum frequency generation process in the electronically excited state of a model molecular system.

Introduction

Sum frequency generation (SFG) is the second-order nonlinear process when two optical waves at frequencies of ω_1 and ω_2 interact simultaneously with a medium to create a new optical wave at the sum of the two frequencies as $\omega_{SF} = \omega_1 + \omega_2$. Since the early 1980s, it has been established that the SFG process, as well as other second-order nonlinear processes, is interface selective because of the symmetry requirement for the even order optical processes, and SFG has been extensively used as the unique technique for interface spectroscopic studies.[1–5] In SFG vibrational spectroscopy (SFG-VS), usually one overlaps a laser beam with tunable infrared (IR) frequency (ω_2) and a laser beam with a fixed or tunable visible (vis) frequency (ω_1) simultaneously at the molecular interface, and the IR or visible wavelength-dependent response of the sum frequency (ω_{SF}) signal is recorded. When the IR wavelength is in resonance with the vibrational frequencies of the interfacial molecules, the sum frequency spectrum gives the vibrational spectrum of the interfacial molecular species. This process is usually called the singly resonant IR SFG-VS. When both the IR and the visible frequency (ω_1) or the SF frequency (ω) are in resonance with the molecules, the process is call the doubly resonant sum frequency generation (DR-SFG), which can be used to probe both the vibrational and the electronic spectra, as well as the coupling effect between the vibrational and electronic motions, of the interfacial molecular species. In the literature, both the IR−visible(ω) processes (i.e., the IR and SF frequencies are in resonance) and the IR−visible(ω_1) processes (i.e., the IR and visible frequencies are in resonance) were called the IR−visible DR-SFG.[6–9]

The IR−visible(ω) DR-SFG spectroscopy of Rhodamine 6G molecules at the fused quartz surface was first reported by Shen and co-workers.[6] In this doubly resonant SFG process, the IR wavelength was in resonance with the skeleton vibrational transitions (frequency around 1500−1750 cm^{-1}) in the Rhodamine 6G ground electronic state (S_0), and the SF wavelength was in resonance with the S_0 to S_1 electronic transition (peaked around 530 nm). Therefore, what was observed was the IR−visible(ω) process, instead of the IR−visible(ω_1) process. Shen and co-workers also concluded that because of the ultrafast dephasing time of the vibronic transitions of the Rhodamine 6G molecule in its S_1 state, the visible−IR DR-SFG process that starts with an electronic transition followed by a vibrational transition in the excited S_1 state should have been greatly suppressed; therefore, it was not observable in the DR-SFG experiment.[6] The subsequent theoretical studies on the DR-SFG also agreed with this conclusion.[7]

Previous to this experimental study, a few theoretical articles detailed the molecular theory of the DR-SFG phenomenon.[8,9] There also were several DR-SFG experimental studies in the past few years, and their themes were to utilize the additional enhancement effect and molecular selectivity provided by the double-resonance SFG process to probe molecules at the electrochemical surfaces and in thin films.[10–14] Shen and co-workers also showed that the IR−visible DR-SFG is chiral selective (i.e., the enhancement effect is much more significant for the nonlinear chiral term rather than the achiral terms).[12,15]

Here, we report the observation of the interference effect between the IR−visible(ω_1) and visible(ω_1)−IR processes in the DR-SFG-VS of Rhodamine 6G adsorbed at the air/water interface. This is achieved by using the picosecond visible light at 532.1 nm, which is in resonance with the S_0 to S_1 electronic transition, and the picosecond IR light at 2800−3100 cm^{-1}. The previously believed to be unexpected visible(ω_1)−IR DR-SFG process appeared as a continuous background that interferes with the IR−visible(ω_1) DR-SFG spectra with discrete spectral features. This same interference effect was also observed for the skeleton vibrational modes in the 1450−1700 cm^{-1} region.

Experimental Section

The DR-SFG spectra of Rhodamine 6G was obtained with a picosecond SFG spectrometer laser system (EKSPLA, Lithua-

* To whom correspondence should be addressed. Telephone: 86-10-62555347. Fax: 86-10-62563167. E-mail: hongfei@iccas.ac.cn.
[†] Graduate University of the Chinese Academy of Sciences.
[‡] Hefei National Laboratory for Physical Sciences at Microscale, University of Science and Technology of China.

10.1021/jp901655j CCC: $40.75
Published on Web 05/07/2009

nia) in a copropagating configuration. The details of the SFG spectrometer were described in the literature.[23,24] The laser pulse width at 532.1 nm is ~23 ps with a repetition rate of 10 Hz, and the IR wavelength is tunable from 2.3 to 10 μm. The spectral resolution of the spectrometer is <6 cm^{-1}, and it is about 2 cm^{-1} around 3000 cm^{-1}. In the experiment, the visible frequency (ω_1) is fixed at 532.1 nm. In the 2800−3100 cm^{-1} region, the incident angles of visible and IR laser beam were 45° and 56°, respectively. Each spectral scan was with 5 cm^{-1} step increment of the IR wavelength. While in the 1450−1700 cm^{-1} region, the incident angles of visible and IR laser beam were 45° and 52°, respectively. The slightly different IR incident angle from 56° as in the 2800−3100 cm^{-1} region has little influence on the SFG intensity.[25] Each spectrum was scanned with a 2 cm^{-1} step increment of the IR wavelength. Each data point was averaged over 200 laser pulses, and each spectrum was repeated and averaged for over five times. The SFG spectra were normalized over the incident IR and visible energies and then normalized with the SFG spectra of a thick z-cut quartz crystal.[26] The incoherent two-photon fluorescence from the solution phase was measured and subtracted. The pulse energy of the visible and IR lights was less than 300 μJ. There was no evidence for heating effect or photoinduced reactions under these experimental conditions.

The Rhodamine 6G dye was purchased from Sigma-Aldrich (laser grade, purity ≈ 99%) and used without further purification. The ultrapure deionized water (18.2 MΩ·cm) used as solvent was from the standard Millipore treatment. In the SFG measurement, the solution sample was filled in a round Teflon beaker (diameter ≈ 5 cm). All experiments were carried out at controlled room temperature (22.0 ± 1.0 °C) and humidity (~40%). The whole system is set on the optical table, and the sample stage was covered in a plastic housing to avoid the air flow. The UV−vis absorption spectra of the Rhodamine 6G aqueous solutions were measured with the UV-1601pc (SHIMADZU, Japan) UV−visible spectrophotometer at ambient condition.

Results and Discussion

Rhodamine 6G, molecular structure as shown in Figure 1, is a widely studied dye molecule because of its broad applications ranging from organic laser dyes to fluorescent tags and biological staining agents. Many experimental techniques and theoretical methods have been used to investigate the physical and chemical properties of R6G in diverse environments. These include techniques such as surface-enhanced Raman scattering,[16] doubly resonant SFG,[6] second harmonic generation,[17] UV−vis absorption spectroscopy and fluorescence emission spectroscopy,[18,19] molecular dynamic simulation,[20] density functional theory,[21] and so forth. In dilute aqueous solution, R6G broadly absorbs light from 430 to 580 nm (peaks around 530 nm) in the visible region, and it fluoresces intensely around 555 nm.[18,19,22]

Figure 2 shows the measurement of the weak SFG signal against the strong two-photon fluorescence (TPF) background longer than 500 nm. The TPF extended into much shorter wavelengths as the detection sensitivity was increased to measure the weak SFG signal. Even though in SFG measurement the SF frequency is well separated from the one-photon florescence, the issue of overlapping TPF background with the SFG signal is especially important when measuring the weak SFG from fluorescent chromophores which can have significant two-photon absorption cross sections.[27,28] In this study, the TPF from the Rhodamine 6G was carefully subtracted as the IR beam was blocked, as illustrated in the inset in Figure 2. Then, it is

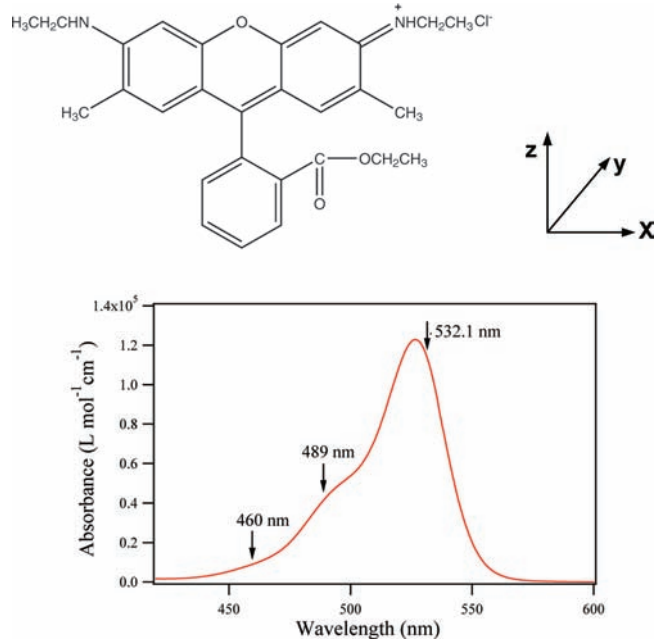

Figure 1. Top: Molecular structure of Rhodamine 6G. The transition dipole of the S_0 to S_1 transition peaked around 527 nm is along the x direction in the molecular frame. Bottom: Absorption spectrum of the Rhodamine 6G aqueous solution. Both the visible frequency (ω_1) at 532.1 nm and the two SFG frequencies (ω_{SF}) at 489 nm (corresponding to the 1653 cm^{-1} skeleton vibration peak) and 460 nm (corresponding to the 2948 cm^{-1} C−H stretching vibration peak) are in resonance with the S_0 to S_1 transition of the Rhodamine 6G. Therefore, they are both doubly resonant SFG processes.

rather strange to find that there was detectable SFG signal observed when the IR frequency is at $\omega_2 = 3000$ cm^{-1} (SFG wavelength at 458 nm), which is not in resonance with any known molecular vibrations. However, this was undoubtedly a SFG signal because when the IR beam was blocked the peak at 458 nm disappeared and only the continuous background remained unchanged.

Figure 3 shows the SFG spectra in the 2800−3100 cm^{-1} region from the interface of 1 and 5 mM Rhodamine 6G aqueous solutions in the ssp, ppp, and sps polarizations. The SFG signal reached saturation at 1 mM, indicating a full Gibbs monolayer is reached around this bulk concentration. In general, the SFG vibrational spectra from various interfaces can be described with the following expression:[4,5]

$$\chi^{(2)}_{ijk} = \chi^{(2)}_{NR,ijk} + \sum_q \frac{\chi_{q,ijk}}{\omega_2 - \omega_q + i\Gamma_q} \qquad (1)$$

Here, $\chi^{(2)}_{NR,ijk}$ represents the nonresonant term, and the sum includes all the vibrationally resonant terms. $\chi_{q,ijk}$, ω_q, and Γ_q represent the sum frequency strength factor tensor, resonant frequency, and damping constant of the qth molecular vibrational mode, respectively. For dielectric interfaces, such as liquid interfaces, the nonresonant term $\chi^{(2)}_{NR,ijk}$ is usually negligible compared with the resonant terms. For metal interface, $\chi^{(2)}_{NR,ijk}$ is usually imaginary and can be comparable to or significantly larger than the resonant terms. However, the SFG data in Figure 3 is clearly an exception. Four typical line shapes using eq 1 when χ_{NR} is nonzero are illustrated in Figure 4.

Comparing the shape of the ssp spectra in Figure 3 with the simulation in Figure 4d, we expect that the imaginary part of the nonresonant term χ_{NR} has the same sign as the resonant term χ_q of the 2950 cm^{-1} negative peak (i.e., the continuous background has the same phase as that of the 2950 cm^{-1} peak)

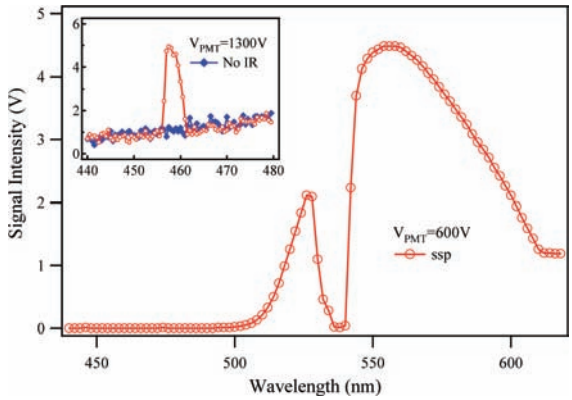

Figure 2. Emission spectra when the IR and visible wavelength are fixed. The strong two-photon fluorescence background from the 1 mM Rhodamine 6G aqueous solution was measured when the IR beam was blocked. The big dip centered at 532.1 nm was caused by the use of the notch filter in the detection system to block the strong scattered light at 532.1 nm from the incident laser beam. The inset contains the emission spectrum with the ssp SFG signal at 458 nm (i.e., when $\omega_2 = 3000\ cm^{-1}$) and a significant fluorescence background, indicated by the data points when IR is blocked. Here the polarization combination ssp denotes the polarization combinations of the SFG signal field (s polarization), the incident visible field (s polarization), and the incident IR field (p polarization). p denotes that the optical field vector is within the incident plane in the experimental configuration, and s means the field vector is perpendicular to this incident plane. The visible incident angle is 45°, and IR incident angle is 56°. This significant fluorescence background has to be subtracted from the measured signal in obtaining the SFG spectra shown in Figure 3. To measure the weak SFG signal, the bias voltage of the PMT was set at 1300 V instead of 600 V for measuring the strong fluorescence. There is a gain difference of 200 for the two voltages.

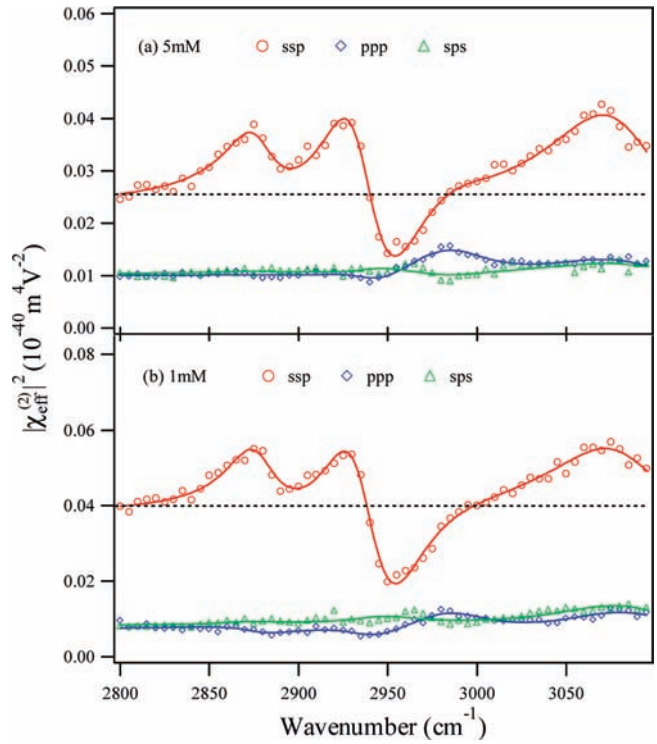

Figure 3. C−H stretching vibrational SFG spectra at the air/R6G aqueous solution interface with bulk R6G concentrations at 5 and 1 mM. The solid lines are fitting curves with multiple Lorentzian lines. The peak positions from fitting (Table 1) do not necessarily coincide with the apparent peaks or valleys in the spectra because of the interference effect with the continuous background. The dashed horizontal line is to guide the eye for the continuous background in the ssp polarization combination.

and the absolute value of χ_{NR} is bigger than that of χ_q/Γ_q. The fitting results in Table 1 confirm this. Apparently, the spectra in Figure 3 all have nonzero backgrounds, and there are apparent interference features around the C−H stretching vibrational frequencies at 2870, 2930, 2950, 2980, and 3070 cm^{-1}. The nonzero background is more than 1 order of magnitude stronger than the SFG signal from the neat air/water interface in the 2800−3000 cm^{-1} region, which is less than 1×10^{-43} m^4 V^{-2}.[30] We also performed SFG experiments on the 5 mM Rhodamine 6G D_2O solution surface in the 2800−3800 cm^{-1} region, and the magnitude of the continuous background as well as the interference pattern in the 2800−3100 cm^{-1} region were the same as those from the Rhodamine 6G H_2O solution surface.[31] Therefore, the continuous background and the interference pattern in the SFG data cannot be attributed to the interfacial water molecules at the Rhodamine 6G solution surface. The SFG spectra can only be fitted with a complex constant with a negative imaginary part for the nonresonant term $\chi^{(2)}_{NR,ijk}$.

Even though the complex number for nonresonant term $\chi^{(2)}_{NR,ijk}$ is a characteristic of the SFG spectrum of molecules adsorbed on a metal substrate,[5,29] here the Rhodamine 6G at the air/water interface clearly presents the same characteristics. However, such an interference pattern is not expected for a liquid interface where no metallic or other nonlinear substrate is present.[5,32] The SFG spectra from molecules adsorbed on the metallic substrates are usually very strong in the ppp polarization combination,[5] but the polarization dependence of the continuous coherent background is clearly not the same. With all the above, the unexpected interference phenomenon has to be intramolecular (i.e., has to come from the Rhodamine 6G molecule adsorbed on the air/water interface). It is well-known that optical interference effect can only occur when two or more coherent processes are involved. The interference features in the SFG spectra, especially the negative and asymmetrically shaped peak around 2950 cm^{-1} in the ssp spectra, make it impossible to

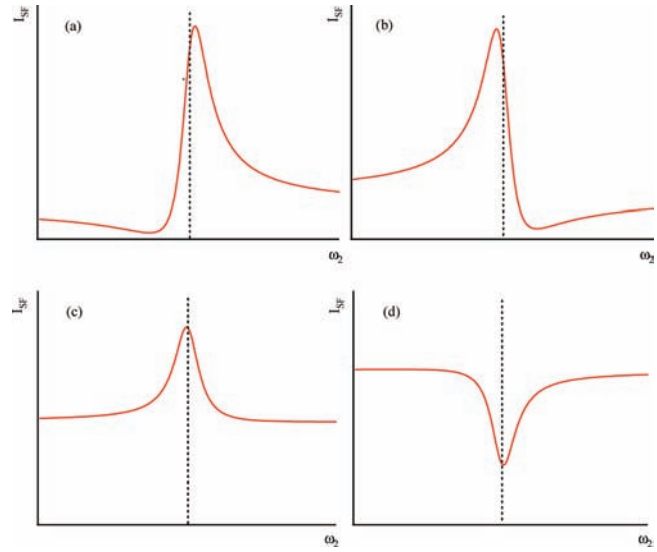

Figure 4. Simulated single peak SFG spectral line shapes with eq 1 when χ_{NR} is nonzero. (a) χ_{NR} is real and has the same sign as χ_q. (b) χ_{NR} is real and has the opposite sign as χ_q. (c) χ_{NR} is imaginary and has the opposite sign as χ_q, with $|\chi_{NR}| > |\chi_q/\Gamma_q|$. (d) χ_{NR} is imaginary and has the same sign as χ_q, with $|\chi_{NR}| > |\chi_q/\Gamma_q|$.[29] The vertical dash line marks the position of the center wavelength (ω_q) of the Lorentzian. One can see that case (d) gives the line shape around 2950 cm^{-1} as observed in Figure 3, while case (c) gives the line shape of the rest peaks as observed in Figure 3.

TABLE 1: Fitting Parameters of the ssp Data from Figure 3, Which Include the Vibrational Peaks Position (ω_q), Width (Γ_q), and Strength Factor of the Nonresonant (χ_{NR}) and Resonant (χ_q) Terms of the Effective Second-Order Susceptibility[a]

ω_q (cm^{-1})		2877.0(1.4)	2933.9(1.6)	2947.7(4.3)	2989.0(5.2)	3080.4(3.0)
Γ_q (cm^{-1})	χ_{NR}	17.1(1.4)	21.2(1.9)	29.1(2.3)	30.0 ± 7.1	39.3(2.4)
χ_q (5 mM)	−0.087(0.015) −0.117(0.015)i	0.61(0.07)	2.82(1.14)	−2.95(1.31)	0.33(0.18)	2.50(0.43)
χ_q (1 mM)	−0.091(0.020) −0.168(0.015)i	0.68(0.08)	3.06(1.35)	−3.74(1.56)	0.08(0.14)	1.85(0.27)

[a] The 5 and 1 mM ssp data were fitted using a global fitting procedure with five Lorentzian peaks. The errors for the fitting parameters are given in parentheses.

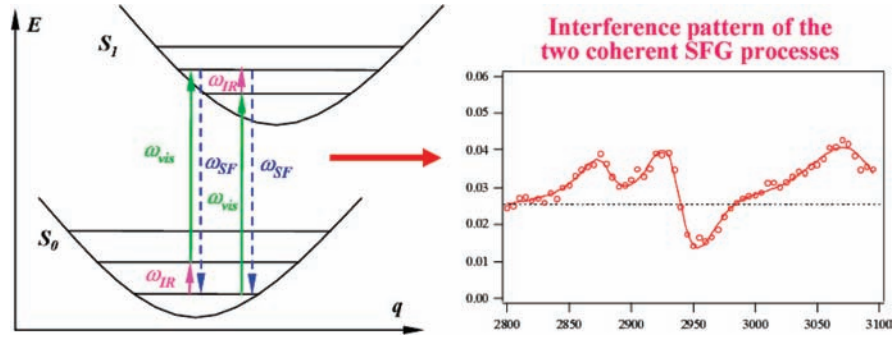

Figure 5. Coherent interference between the two visible(ω_1)−IR and IR−visible(ω_1) SFG processes is considered to be the mechanism for the observed SFG spectra for the Rhodamine 6G at the air/water interface.

attribute the strong nonzero background to any incoherent processes, such as the two-photon fluorescence that was already removed from the data. The existence of a continuous coherent background in the SFG spectra also explains the significant vibrationally nonresonant SFG signal at 458 nm (ω_2 = 3000 cm^{-1}) as observed in Figure 2.

Then what can be the origin of this unexpected coherent process? In Figure 1, we can see that both the 532.1-nm visible light and the SFG wavelength for the C−H stretching vibrations around 460 nm are in the S_0 to S_1 absorption band. This suggests that the visible(ω_1)−IR SFG process is the most likely explanation for the significant continuous coherent background. Because of the continuous vibronic band structure associated with the ultrafast dephasing dynamics of the S_1 state, the visible(ω_1)−IR process can result in a continuous SFG spectrum. To further support this picture, the complex $\chi^{(2)}_{NR,ijk}$ term also suggested that a continuous, or very broad, electronic transition similar to the plasmon resonance in the metallic materials should be involved. Indeed, previous femtosecond experiments found that the vibrational relaxation time of the excited states of the Rhodamine 6G was less than 30 fs.[33,34] This ensures that its S_1 to S_0 electronic transition is a very broad spectrum to support the continuous visible(ω_1)−IR process. Consequently, the interference between this visible(ω_1)−IR process with a continuous spectrum and the IR−visible process with a discrete spectrum can produce the SFG spectra as observed. The proposed mechanism of the interference between the two kinds of SFG processes is illustrated in Figure 5.

If this mechanism is true, the continuous visible(ω_1)−IR SFG spectra and spectral interference must be also observable for the skeleton vibrations whose SFG wavelength is around 489 nm, which is also located in the middle of the S_0 to S_1 absorption band for Rhodamine 6G. However, such interference effect was not observed or predicted in the previous DR-SFG studies.[6,7]

Figure 6 presents the SFG spectra at the air/R6G aqueous solution (5 mM) interface in the ssp polarization combination in the C−C−C skeleton vibration region (1450−1700 cm^{-1}). The spectrum for the 1 mM solution was very similar and is not presented here. The $|\chi_{eff}^{(2)}|^2$ values measured here are

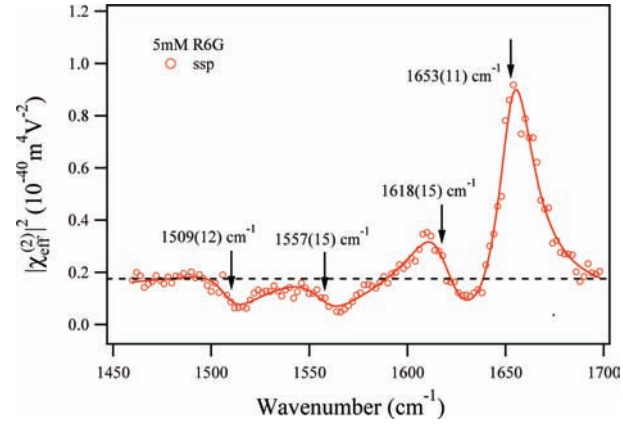

Figure 6. SFG spectra at the air/R6G aqueous solution (5 mM) interface in ssp polarization in the C−C−C skeleton vibrational region (1460−1700 cm^{-1}) with visible wavelength as 532.1 nm. The solid lines are fitting curves with multiple Lorentzian lineshapes. The four vibrational peak positions and spectral bandwidth (Γ) from fitting results (Table 2) are labeled in the graph.[29] The peak positions do not necessarily coincide with the apparent peaks or valleys in the spectra because of the interference effect with the continuous background. The dashed horizontal line is to guide the eye for the continuous background.

consistent with the $|\chi_{eff}^{(2)}|^2$ values in the literature measured at the similar visible wavelengths of Rhodamine 6G adsorbed on the fused silica substrate surface,[6] indicating the spin-coated Rhodamine 6G film in the previous study was approximately with single layer coverage. The nonzero baseline in the spectrum in Figure 6 well exceeds the detection sensitivity (about 1 × 10^{-43} m^4 V^{-2}) in the experiment. However, it was well below the noise level (in the order of 1 × 10^{-40} m^4 V^{-2}) in Shen and co-workers' DR-SFG experiment, where the intensity of the ω_1 = 532.1 nm SFG spectrum is more than 20 times smaller than that of the ω_1 = 590 nm spectrum.[6] Even though in the singly resonant SFG measurement of the O−H spectra at the air/water interface the $|\chi_{eff}^{(2)}|^2$ sensitivity of 1 × 10^{-43} m^4 V^{-2} can be achieved,[26,29,35] such sensitivity was not pursued in the previous DR-SFG study on Rhodamine 6G.[6]

TABLE 2: Fitting Parameters of the Data from Figure 6 Using Four Lorentzian Peaks, Which Include the Vibrational Peak Position (ω_q), Peak Width (Γ_q), and Strength Factor of the Nonresonant (χ_{NR}) and Resonant (χ_q) Terms of the Effective Second-Order Susceptibility[a]

ω_q (cm^{-1})		1509.0(1.7)	1557.0(1.7)	1618.1(1.3)	1653.3(0.5)
Γ_q (cm^{-1})	χ_{NR}	11.9(2.8)	15.1(3.4)	14.8(1.8)	11.3(0.3)
χ_q	$-0.066(0.009)$ $+0.334(0.016)$i	2.14(0.47)	3.05(0.69)	8.7(1.5)	12.95(0.62)

[a] The errors for the fitting parameters are given in parentheses.

Fitting of the spectrum in Figure 6 can be achieved using eq 1 with a complex $\chi^{(2)}_{NR,ijk}$ term with a positive imaginary part. The fitting parameters are listed in Table 2. Similar to the case for the negative peak at 2950 cm^{-1}, the continuous background has the same phase with the vibrational peaks at 1509 and 1557 cm^{-1}, which both appeared as negative peaks in the SFG spectra. However, as the nonresonant term $|\chi_{NR}|$ becomes smaller than $|\chi_q/\Gamma_q|$, the vibrational peaks become positive above the baseline as the 1618 and 1653 cm^{-1} peaks in Figure 6. From the fitting results in Tables 1 and 2, the imaginary part of χ_{NR} in the 1450−1700 cm^{-1} region is positive, but it is negative in the 2800−3100 cm^{-1} region. However, the signs of these two χ_{NR} terms are relative to the phases of the vibrational peaks in the different regions, and they cannot be compared directly. This can be resolved if additional absolute phase measurement is conducted in future work. Nevertheless, the peak positions and the damping constants (Γ) of the four vibrations in the 1450−1700 cm^{-1} region are fully consistent with the previously reported results for the skeleton vibrations.[6] These results confirmed the existence of the continuous coherent background in the skeleton vibration region (1450−1700 cm^{-1}). Unlike the $\omega_1 = 532.1$ nm case, the $\omega_1 = 590$ nm is not in resonance with the S_0 to S_1 electronic transition of the Rhodamine 6G molecule. Thus, the interference phenomenon with the visible(ω_1)−IR process cannot be observed in the $\omega_1 = 590$ nm SFG spectrum as in the previous article by Shen et al.[6]

From Figure 3 we can see that the magnitude of the visible(ω_1)−IR process, which appeared as the continuous coherent background in the SFG spectra, is several times larger than that of the IR−visible(ω_1) process, which appeared as the peaks and valleys in the SFG spectra; from Figure 4 the magnitude of the visible(ω_1)−IR process is only comparable or much smaller than the IR−visible(ω_1) process. Such difference between the strength of the interfering IR−visible(ω_1) process and visible(ω_1)−IR process for the two vibrations can be understood by the difference of the different coupling strengths between the vibrational transition and the electronic transition, respectively. Since the S_0 to S_1 electronic transition in the Rhodamine 6G molecule is localized in the skeleton region, the CH_2 and CH_3 stretching modes in the ground electronic state located outside the Rhodamine 6G skeleton are only weakly coupled to the S_0 to S_1 electronic transition, while the coupling between the skeleton vibrations in the electronic ground state and the S_0 to S_1 electronic transition is much stronger.[6,7] Comparison of the resonance Raman and the off-resonance Raman spectral intensities of the CH_2 and CH_3 stretching modes and the skeleton modes can directly give information on their relative coupling strengths. However, as pointed out by Jensen and Schatz and others,[36] it is not possible experimentally to obtain the RRS spectrum of R6G at a wavelength around 530 nm because of strong fluorescence. On the other hand, according to the off-resonance Raman spectra of the Rhodamine 6G,[37] the intensities of the skeleton modes around 1300−1700 cm^{-1} were indeed 1 order of magnitude larger than those of the CH_2 and CH_3 stretching modes around 2800−3000 cm^{-1}. According to the fitting results in Tables 1 and 2, the susceptibility value of the electronically weakly coupled C−H stretching vibrations is smaller than that of the electronically coupled skeleton vibrations. The interference effect with the much larger continuous coherent background from the visible(ω_1)−IR process actually significantly amplified these vibrational features in the total SFG spectra. Otherwise, these C−H stretching vibrational features would be barely detectable with the 1×10^{-43} m^4 V^{-2} detection sensitivity. Therefore, the existence of the interfering visible(ω_1)−IR process can be employed to amplify the very weak IR−visible(ω_1) signal in a future DR-SFG experiment. This can be especially useful when the density of the interfacial molecule is at the submonolayer level and the total IR−visible(ω_1) SFG response is expected to be small.

As in Figures 3 and 6, the magnitude of the visible(ω_1)−IR process in the 2800−3100 cm^{-1} region (i.e., the level of continuous coherent background) is also several times weaker than that of the visible(ω_1)−IR process in the 1450−1700 cm^{-1} region. This can be readily understood by the relative absorption spectral intensities of the SFG wavelengths of these two processes (i.e., around 460 nm versus 489 nm, respectively), as labeled in the absorption spectrum of the Rhodamine 6G in Figure 1. The spectral density at 489 nm is about four or five times larger than that at 460 nm in the absorption spectra. Therefore, the SFG susceptibility of the former process is expected to be significantly larger than that for the latter. The relative phase between the continuous backgrounds for the SFG spectra around 460 and 489 nm can be determined through SFG phase measurement. This can provide further information on the details of the molecular orientation and spectral coupling. These warrant further investigations in the future.

One direct way to confirm the visible−IR SFG process is to vary the visible wavelength when the IR wavelength is fixed to see whether the spectral response of the continuous background in the SFG signal follows the S_0 to S_1 electronic transition spectrum. However, this experiment requires the sensitivity of the current DR-SFG, which is normally about 2 orders of magnitude less sensitive for the same small SFG signal level than the fixed visible wavelength SFG experiment, to be improved by at least 1 to 2 orders of magnitude for the Rhodamine 6G system.[6] This shall be pursued in future studies. In addition to Rhodamine 6G, a strong continuous coherent background was also observed in the DR-SFG-VS spectra of the Coumarin 314 dye molecule adsorbed at the air/water interface in our laboratory.[31] The detailed analysis and comparison to the data for both the DR-SFG-VS of the interfacial Rhodamine 6G and Coumarin 314 molecules shall be presented in the near future.

Conclusions

In conclusion, the interference effects between the intramolecular IR−visible and visible−IR processes in the doubly resonant sum frequency generation vibrational spectroscopy of

Rhodamine 6G adsorbed at the air/water interface were observed. The interference phenomenon exists for both the C−H stretching vibrations in the 2800−3100 cm^{-1} region and the skeleton vibrations in the 1450−1700 cm^{-1} region. The relative strength of the visible−IR process at different wavelengths depends on the electronic structure of the molecule. The magnitude of the visible−IR DR-SFG process is larger than that of the IR−visible DR-SFG of the weakly electronically coupled vibrational modes (C−H stretching modes), but smaller than that of the strongly electronically coupled vibrational modes (skeleton modes).

This is the first direct observation of the visible−IR SFG process in the electronically excited state of a model molecular system. According to the same general principle, the visible−IR process as well as its interference with the IR−visible process are expected to be commonly observable in the DR-SFG processes. Recently, the development of the multiplex SFG technique for measuring both the vibrational and the electronic responses of interfacial molecules is going to find broad applications in the DR-SFG surface studies.[38] The phenomenon as observed in this work may provide an effective probe for the electronically excited states of the molecules at the molecular interfaces, as well as in the ordered molecular systems.

Acknowledgment. D.W. thanks Yuan Wang for helpful discussions. H.F.W. thanks the Natural Science Foundation of China (No. 20425309, No. 20533070, No. 20773143) and the Ministry of Science and Technology of China (No. 2007CB815205) for support. Y.G. also thanks the Natural Science Foundation of China (No. 20673122) for support.

References and Notes

(1) Shen, Y. R. *Nature* **1989**, *337*, 519–525.
(2) Eisenthal, K. B. *Chem. Rev.* **1996**, *96*, 1343–1360.
(3) Bain, C. D. *J. Chem. Soc., Faraday Trans.* **1995**, *91*, 1281–1296.
(4) Wang, H. F.; Gan, W.; Lu, R.; Rao, Y.; Wu, B. H. *Int. Rev. Phys. Chem.* **2005**, *24*, 191–256.
(5) Buck, M.; Himmelhaus, M. *J. Vac. Sci. Technol., A* **2001**, *19*, 2717–2736.
(6) Raschke, M. B.; Hayashi, M.; Lin, S. H.; Shen, Y. R. *Chem. Phys. Lett.* **2002**, *359*, 367–372.
(7) Hayashi, M.; Lin, S. H.; Raschke, M. B.; Shen, Y. R. *J. Phys. Chem. A* **2002**, *106*, 2271–2282.
(8) Lin, S. H.; Hayashi, M.; Islampour, R.; Yu, J.; Yang, D. Y.; Wu, Y. C. *Physica B* **1996**, *222*, 191–208.
(9) Huang, J. Y.; Shen, Y. R. *Phys. Rev. A* **1994**, *49*, 3973–3981.
(10) Bozzini, B.; D'Urzo, L.; Mele, C.; Busson, B.; Humbert, C.; Tadjeddine, A. *J. Phys. Chem. C* **2008**, *112*, 11791–11795.
(11) Li, Q. F.; Hua, R.; Chou, K. C. *J. Phys. Chem. B* **2008**, *112*, 2315–2318.
(12) Belkin, M. A.; Shen, Y. R. *Phys. Rev. Lett.* **2003**, *91*, 213907.
(13) Busson, B.; Tadjeddine, A. *J. Phys. Chem. C* **2008**, *112*, 11813–11821.
(14) Humbert, C.; Busson, B.; Six, C.; Gayral, A.; Gruselle, M.; Villain, F.; Tadjeddine, A. *J. Electroanal. Chem.* **2008**, *621*, 314–321.
(15) Belkin, M. A.; Shen, Y. R. *Int. Rev. Phys. Chem.* **2005**, *24*, 257–299.
(16) Hildebrandt, P.; Stockburger, M. *J. Phys. Chem.* **1984**, *88*, 5935–5944.
(17) Heinz, T. F.; Chen, C. K.; Ricard, D.; Shen, Y. R. *Phys. Rev. Lett.* **1982**, *48*, 478–481.
(18) Selwyn, J. E.; Steinfeld, J. I. *J. Phys. Chem.* **1972**, *76*, 762–774.
(19) Toptygin, D.; Packard, B. Z.; Brand, L. *Chem. Phys. Lett.* **1997**, *277*, 430–435.
(20) Daré-Doyen, S.; Doizi, D.; Guilbaud, Ph.; Djedaïni-Pilard, F.; Perly, B.; Millié, Ph. *J. Phys. Chem. B* **2003**, *107*, 13803–13812.
(21) Gavrilenkoa, V. I.; Noginov, M. A. *J. Chem. Phys.* **2006**, *124*, 044301.
(22) Nakashima, K.; Duhamel, J.; Winnik, M. A. *J. Phys. Chem.* **1993**, *97*, 10702–10707.
(23) Lu, R.; Gan, W.; Wu, B. H.; Chen, H.; Wang, H. F. *J. Phys. Chem. B* **2004**, *108*, 7297–7306.
(24) Lu, R.; Gan, W.; Wu, B. H.; Zhang, Z.; Guo, Y.; Wang, H. F. *J. Phys. Chem. B* **2005**, *109*, 14118–14129.
(25) Gan, W.; Wu, B. H.; Chen, H.; Guo, Y.; Wang, H. F. *Chem. Phys. Lett.* **2005**, *406*, 467–473.
(26) Gan, W.; Wu, D.; Zhang, Z.; Feng, R. R.; Wang, H. F. *J. Chem. Phys.* **2006**, *124*, 114705.
(27) Dreesen, L.; Humbert, C.; Sartenaer, Y.; Caudano, Y.; Volcke, C.; Mani, A. A.; Peremans, A.; Thiry, P. A.; Hanique, S.; Frère, J. M. *Langmuir* **2004**, *20*, 7201–7207.
(28) Rao, Y.; Guo, X. M.; Tao, Y. S.; Wang, H. F. *J. Phys. Chem. A* **2004**, *108*, 7977–7982.
(29) Miranda, P. B.; Shen, Y. R. *J. Phys. Chem. B* **1999**, *103*, 3292–3307.
(30) Bian, H. T.; Feng, R. R.; Xu, Y. Y.; Guo, Y.; Wang, H. F. *Phys. Chem. Chem. Phys.* **2008**, *10*, 4920–4931.
(31) Unpublished data, Hong-fei Wang group, Institute of Chemistry, the Chinese Academy of Sciences, 2008.
(32) Ostroverkhov, V.; Waychunas, G. A.; Shen, Y. R. *Phys. Rev. Lett.* **2005**, *94*, 046102.
(33) Shank, C. V.; Ippen, E. P.; Teschke, O. *Chem. Phys. Lett.* **1977**, *45*, 291–294.
(34) Taylor, A. J.; Erskine, D. J.; Tang, C. L. *Chem. Phys. Lett.* **1984**, *103*, 430–435.
(35) Wei, X.; Shen, Y. R. *Phys. Rev. Lett.* **2001**, *86*, 4799–4802.
(36) Jensen, L.; Schatz, G. C. *J. Phys. Chem. A* **2006**, *110*, 5973–5977.
(37) Off-resonance FT-Raman spectra of Rhodamine 6G taken with excitation wavelength of 1064 nm with Nicolet Raman 950 spectrometer was from the Aldrich Raman Condensed Phase Spectral Library.
(38) Ishibashi, T.; Onishi, H. *Appl. Phys. Lett.* **2002**, *81*, 1338–1340.

JP901655J